Original Research Article

A Hydrodynamic Model of Flow in a Bifurcating Stream, Part 1: Effects of Bifurcation Angle and Magnetic Field

Abstract A hydrodynamic model of the flow in a bifurcating stream is presented. The problem is modeled using the Boussinesq approximations, and the governing nonlinear equations solved analytically by the methods of similarity transformation and regular perturbation series expansions. The similarity expressions for the temperature, concentration and velocity are obtained and analyzed graphically. The results show that bifurcation angle and Reynolds number increase the transport velocity. Furthermore, it is seen that the magnetic field parameter decreases the velocity in the upstream region, and makes it oscillatory in the downstream region.

Keywords: bifurcation, hydrodynamic model, magnetic field, porous, perturbation method, similarity transformation, stream

1 INTRODUCTION

The strength depends on its mass-volume and velocity, and its velocity, amongst others, depends on the difference in gradient between its source in the mountain and mouth in a standing water body ([1], [2]). Based on the slope differential, a stream can be divided into three regions: the erosion (upper or torrent) zone; the transfer (middle or valley) zone, and the depositional zone. In the erosion zone, the stream flows through a deep descent; therefore, its velocity is very high and the flow very erosive. It vertically down-cuts and removes the bed rocks from the valley floor and sides. In the mid-valley course, the gradient is lower than that of the upper course and so is the velocity but it is able to carry the eroded materials and rocks farther. In the depositional course, the gradient is very low and so is the flow such that the rate of deposition of materials on the stream bed, and on the flood plain during flood is very high.

Several features like the braided streams (or rivers), anastomosing stream, meanders and the likes are formed in the depositional zone ([1], [2]). In particular, anastomosing rivers represent a type of rivers that are currently of interest in geomorphology and sedimentology. They have multiple inter-connected channels separated by areas of the flood plains. Usually, in the tropical region, the river banks are stabilized by vegetation and in the arid region by highly consolidated rocks. They help to inhibit lateral migration of channels. However, at points where the banks have loose structures, the stream may suddenly abandon its old course for a new course or part of its old course to form a by-pass. At the points of the by-pass, the river is said to divide or anastomose ([1], [2]).

Many techniques have been employed for studying the flow dynamics of the stream. Some used the hydrologic model, which involves the use of spatial form of the continuity equation or water balance and flux relation expressing storage as a function of inflow and outflow (see [4]); some the hydraulic model, which is based on the use of St. Venant equations (see [5]), and others the stochastic probability model, which involves the use of Monte Carlo method (see [3], [6]). In very recent time, [7] presented a 2-D hydrodynamic model using TELEMAC-2D software for flood simulation in a river. From the available literatures, it is evident that there is very scanty number of hydrodynamic models on stream flow. Therefore, we are motivated to present a hydrodynamic model for flow in a bifurcating stream.

Research workers have done some work on the flow in bifurcating systems. For example, [8], [9], [10], [11], [12], [13] and [14] examined numerically and experimentally the flow structure in bifurcating systems and observed that bifurcation angle increases the inlet pressure and subsequently increases the flow velocity of such systems.

Apart from the gradient differential, dynamically, a number of factors affect the flow of the stream. Based on this, the purpose of this paper is to investigate the effects of bifurcation angles and the nature of the source rocks on the flow of a bifurcating stream.

This paper is organized in the following manner: section 2 is the methodology; section 3 holds the results; section 4 is the discussion of results, and section 5 holds the conclusions.

2 METHODOLOGY

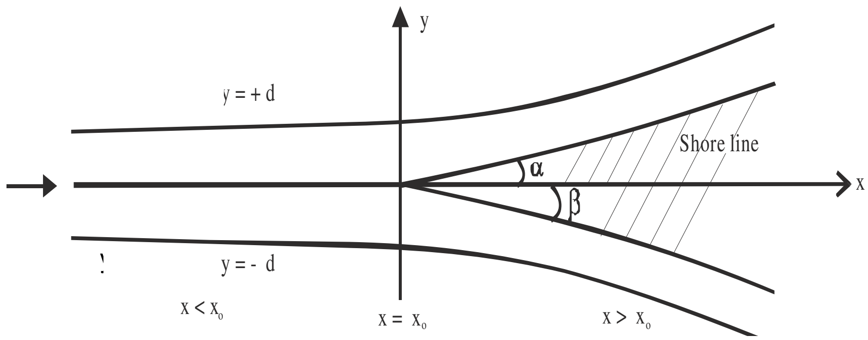

Figure 1 A physical model of symmetrical bifurcating flowing stream.

The stream is approximately rectangular in form and planar at the surface. We assume that the flow is axi-symmetrical about the z-axis; due to the nature of the source rock the fluid is magnetically susceptible, and incompressible and Newtonian; the fluid viscosity is a function of temperature and magnetic field; the fluid is chemically reacting, and of a homogeneous first order type (i.e. the reaction is proportional to the concentration); the porous medium is non-homogeneous, therefore, its permeability is anisotropic; the fluid have constant properties except that the density varies with the temperature and concentration which are considered only in the force term. If (u', v') are respectively the velocity components of the fluid in the mutually orthogonal (x', y') axes, the mathematical equations of mass balance/continuity, momentum, energy and diffusion governing the flow in the presence of bifurcation, and considering the Boussinesq and Swell's free flow in vector form become:

$$\nabla . v' = 0 \tag{1}$$

$$\left(v'.\nabla\right)v' = \frac{-1}{\rho}\nabla p' + \frac{\mu}{\rho}\nabla^2 v' + g\beta_t\left(T' - T_\infty\right) + g\beta_c\left(C' - C_\infty\right) - \frac{\mu}{\rho\kappa}v' - \frac{\sigma_e B^2{}_o v'}{\rho^2 \mu\mu_m} \tag{2}$$

$$\left(v'.\nabla\right)T' = \frac{k_o}{\rho C_p}\nabla^2 T' + \frac{Q}{\rho C_p}\left(T' - T_\infty\right) \tag{3}$$

$$\left(v'.\nabla\right)C' = D\nabla^2 C' + k^2{}_r\left(C' - C_\infty\right) \tag{4}$$

where β_t and β_c are the volumetric expansion coefficient for temperature and concentration respectively; C_∞ concentration at equilibrium; T_∞ temperature at equilibrium; κ is the permeability parameter of the porous medium; B_o^2 is the applied uniform magnetic field strength due the nature of the fluid; σ_e is the electrical conductivity of the fluid; k_o the thermal conductivity; C_p the specific heat capacity at constant pressure; Q is the heat absorption coefficient; D the diffusion coefficient; k_r^2 is the rate of chemical reaction of the fluid, which is homogeneous and of order one; C' concentration (quantity of material being transported); D diffusion coefficient; **g** gravitational field vector; p' pressure; T' fluid temperature; ρ density of the fluid; μ viscosity of the fluid; μ_m magnetic permeability of the fluid; υ kinematic viscosity; k_o thermal conductivity of the medium; T_∞ temperature at equilibrium; C_∞ concentration at equilibrium.

The problem examines the dynamics of a bifurcating stream flowing from a point $x' = -\infty$ towards a shore at $x' = x_o$, as seen in Figure 1. The model shows that the channel is assumed to be symmetrical and divided into two regions: the upstream (or mother) region $x' < x_o$ and downstream (or daughter) region $x' > x_o$, where x_o is the bifurcation or the nodal point, which is assumed to be the origin such that the stream boundaries become $y' = \pm d$ for the upstream region and $y' = \alpha x'$ for the downstream region. Due to geometrical transition between the mother and daughter channels, the problem of wall curvature effect is bound to occur. To fix up this, a very simple transition wherein the width of the daughter channel is made equal to half *that* of the mother channel i.e. $\pm d$ such that the variation of the bifurcation angle is straight-forwardly used (see [14]). Furthermore, if the width of the stream ($2d$) is far less than its length (l_o) before the point of bifurcation such that the ratio of $\frac{2d}{l_o} = \Re << 1$, (where $\Re$ is the aspect ratio), the flow is laminar and Poiseuille (see [15]). d is assumed to be non-dimensionally equal to one (see [14]). Similarly, at the entry region of the mother channel, the flow velocity is given as $u' = U_o\left(1 - y'^2\right)$, where U_o is the characteristic velocity, which is taken to be maximum at the centre and zero at the wall (see [14]). Based on the fore-going, the boundary conditions are:

$$u'=1,\ v'=0,\ T'=1,\ C'=1 \quad \text{at} \quad y'=0 \tag{5}$$

$$u'=0,\ v'=0,\ T'=T_w,\ C'=C_w \quad \text{at} \quad y'=1 \tag{6}$$

for the mother channel

$$u'=0,\ v'=0,\ T'=0,\ C'=0 \quad \text{at} \quad y'=0 \tag{7}$$

$$u'=0,\ v'=0,\ T'=\gamma T_w,\ C'=\gamma C_w,\ \gamma_1 < 1,\ \gamma_2 < 1 \ \text{at} \ y'=\alpha x' \tag{8}$$

for the daughter channel

Introducing the following non-dimensional variables:

$$x = \frac{x'}{\ell_c},\ y = \frac{y'}{\ell_c},\ u = \frac{u'}{U_o},\ v = \frac{v'}{U_o},\ p = \frac{p'}{p_\infty},\ \rho_\infty = \rho U_o^2,\ \Theta = \frac{T' - T_\infty}{T_w - T_\infty},\ \Phi = \frac{C' - C_\infty}{C_w - C_\infty},$$

$$\upsilon = \frac{\mu}{\rho},\ \mathrm{Re} = \frac{\rho U_o \ell_c}{\mu},\ Gr = \frac{\rho g \beta_t (T_w - T_\infty)\ \ell_c^2}{\mu U_o}\quad Gc = \frac{\rho g \beta_c (C_w - C_\infty)}{\mu U_o},\ \chi^2 = \frac{\ell_c^2}{\kappa},$$

$$\delta_1^2 = \frac{k_r^2 \ell_c^2}{D},\quad M^2 = \frac{\sigma_e B_o^2\ \ell_c^2}{\rho\mu\mu_m},\ N^2 = \frac{C_p \mu}{k_o},\ Sc = \frac{\mu}{\rho D}$$

where ℓ_c is the scale length, p_∞ is ambient/equilibrium pressure, U_o characteristic or reference velocity which is maximum at the centre and almost zero at the wall, C_w constant wall temperature is maintained, T_w constant wall concentration at which the channel is maintained, ρ_∞ the ambient/equilibrium density, υ is the kinematic viscosity, Re is the Reynolds number, Gr is the Grashof number due to temperature difference, Gc is the Grashof number due to concentration difference, χ^2 is the local Darcy number, M^2 is the Hartmann's number, Pr is the Prandtl number, Sc is the Schmidt number, and δ_1^2 is the rate of chemical reaction, N^2 is the temperature differential into equations (1) - (8),we have

$$\frac{\partial u}{\partial x}+\frac{\partial v}{\partial y}=0 \tag{10}$$

$$\mathrm{Re}\left(u\frac{\partial u}{\partial x}+v\frac{\partial u}{\partial y}\right)=-\frac{\partial p}{\partial x}+\left(\frac{\partial^2 u}{\partial x^2}+\frac{\partial^2 u}{\partial y^2}\right)+Gr\Theta+Gc\Phi-\chi^2 u-M^2 u \tag{11}$$

$$\mathrm{Re}\left(u\frac{\partial v}{\partial x}+v\frac{\partial v}{\partial y}\right)=-\frac{\partial p}{\partial y}+\left(\frac{\partial^2 v}{\partial x^2}+\frac{\partial^2 v}{\partial y^2}\right) \tag{12}$$

$$\mathrm{Re}\,\mathrm{Pr}\left(u\frac{\partial \Theta}{dx}+v\frac{\partial \Theta}{\partial y}\right)=\left(\frac{\partial^2 \Theta}{dx^2}+\frac{\partial^2 \Theta}{\partial y^2}\right)+N^2\Theta \tag{13}$$

$$\mathrm{Re}\,Sc\left(u\frac{\partial \Phi}{dx}+v\frac{\partial \Phi}{\partial y}\right)=\left(\frac{\partial^2 \Phi}{dx^2}+\frac{\partial^2 \Phi}{\partial y^2}\right)+\delta_1^2\Phi \tag{14}$$

with the boundary conditions

$$u = 1,\ v = 0,\ \Theta = 1,\ \Phi = 1 \quad \text{at } y = 0 \tag{15}$$

$$u = 0,\ v = 0,\ \Theta = \Theta_w,\ \Phi = \Phi_w \quad \text{at } y = 1 \tag{16}$$

for the upstream channel

$$u=0,\ v= 0,\ \Theta = 0,\ \Phi = 0 \quad \text{at } y = 0 \tag{17}$$

$$u = 0,\ v = 0,\ \Theta = \gamma_1\Theta_w,\ \Phi = \gamma_2\Phi_w,\ \gamma_1 < 1,\ \gamma_2 < 1 \quad \text{at } y=\alpha x \tag{18}$$

for the downstream channel

Introducing the similarity solution:

$$\Psi = (U_o \upsilon\, x)^{1/2} f(\eta),\ \eta = \left(\frac{U_o}{\upsilon x}\right)^{1/2} y \tag{19}$$

with the velocity components represented as

$$u = \frac{\partial \Psi}{\partial y},\quad v = -\frac{\partial \Psi}{\partial x} \tag{20}$$

into equations (10) - (18), we have the following equivalent equations

$$f'' = 0 \tag{21}$$

$$f''' + f'' - M_1^2 f' + \mathrm{Re}(f'f'' + ff'') = -Gr\,\Theta - Gc\,\Phi \tag{22}$$

$$\Theta'' + \Theta' + \mathrm{Re}\,\mathrm{Pr}(-f'\Theta' + f\,\Theta') + N^2\Theta = 0 \tag{23}$$

$$\Phi'' + \Phi' + R\,eSc(-f'\Phi' + f\,\Phi') + \delta_1^2\Phi = 0 \tag{24}$$

$where\ M_1^2 = (\chi^2 + M^2)$

with the boundary indications:

$$f = 1,\ f' = 0,\ \Theta = 1,\ \Phi = 1 \quad \text{at } \eta = 0 \tag{25}$$

$$f' = 0,\ f = 0,\ \Theta=\Theta_w,\ \Phi=\Phi_w \quad \text{at } \eta = 1 \tag{26}$$

for the upstream channel

$$f = 0,\ f' = 0,\ \Theta = 0,\ \Phi = 0 \quad \text{at } \eta = 0 \tag{27}$$

$$f' = 0,\ f = 0,\ \Theta = \gamma_1\Theta_w,\ \Phi = \gamma_2\Phi_w,\ \gamma_1 < 1,\ \gamma_2 < 1 \quad \text{at } \eta = ax \tag{28}$$

for the downstream channel

Equations (21) - (28) show that the similarity equations are coupled and highly non-linear. Therefore, to minimize the effect of non-linearity on the flow variables we introduce a perturbation series solution of the form

$$h\big(x,y) = h_o(x,y)\big) + \xi h_1(x,y) + \ldots \tag{29}$$

where $\xi = \dfrac{1}{\mathrm{Re}} << 1$ as the perturbing parameter. We choose this parameter because, almost at the point of bifurcation, due to a change in the geometrical configuration, the inertial force rises and the momentum increases. The increase in the momentum is associated with a drastic increase in the Reynolds number, indicating a sort of turbulent flow at such a point . In this regard, equations (21) - (28) become:

for the zeroth order:

$$f_o'' = 0 \tag{30}$$

$$f_o''' + f_o'' - M_1^{\,2} f_o' = -Gr\Theta_o - Gc\Phi_o \tag{31}$$

$$\Theta''_o + \Theta'_o + N^2\Theta_o = 0 \tag{32}$$

$$\Phi_o'' + \Phi_o' + \delta^2{}_1\Phi_o = 0 \tag{33}$$

with the boundary conditions

$$f_o = 1, f_o^{'} = 0, f_o^{''} = 0, \Theta_o = 1, \Phi_o = 1 \quad \text{at} \quad \eta = 0 \tag{34}$$

$$f_o = 0, f_o^{'} = 0, f_o^{''} = 0, \Theta_o = 0, \Phi_o = 0 \quad \text{at} \quad \eta = 1 \tag{35}$$

for the first order:

$$f_1'' = 0 \tag{36}$$

$$f_1''' + f_1'' - M_1^{\,2} f_1^{'} = f_o' f_o'' - f_o f_o'' - Gr\Theta_1 - Gc\Phi_1 \tag{37}$$

$$\Theta_1'' + \Theta_1' + N^2\Theta_1 = \Pr(f_o'\Theta'_o - f_o\Theta'_o) \tag{38}$$

$$\Phi_1'' + \Phi_1' + \delta_1^{\,2}\Phi_1 = Sc(f_o'\Phi_o' - f_o\Phi_o') \tag{39}$$

with the boundary conditions

$$f_1 = 0, f_1^{'} = 0, \Theta_1 = 0, \Phi_1 = 0 \quad \text{at} \quad \eta = 0 \tag{40}$$

$$f_1 = 0, f_1^{'} = 0, \Theta_1 = \gamma_1\Theta_w, \Phi_1 = \gamma_2\Phi_w,\ \gamma_1 < 1, \gamma_2 < 1 \quad \text{at} \quad \eta = ax \tag{41}$$

The zeroth order equations describe the flow in the upstream channel, while the first order equations describe the flow in the downstream channels. The zeroth order terms in the first order equations indicate the influence of the upstream on the downstream flow.

The solutions to equations (30) - (35) and (36) - (41) are:

for the upstream region

$$\Theta_o(\eta) = \frac{\Theta_w e^{\frac{1}{2}(1-\eta)}\sinh\mu_1\eta}{\sinh\mu_1} + \frac{e^{-\frac{1}{2}(1-\eta)}\sinh\mu_1(1-\eta)}{\sinh\mu_1} \tag{42}$$

$$\Phi_o(\eta) = \frac{\Phi_w e^{\frac{1}{2}(1-\eta)}\sinh\mu_2\eta}{\sinh\mu_2} + \frac{e^{-\frac{1}{2}(1-\eta)}\sinh\mu_2(1-\eta)}{\sinh\mu_2} \tag{43}$$

$$f_o(\eta) = \frac{\left(f_{o(p)}(0)e^{-(\mu 3+\eta/2)}\ \sinh\mu_3\eta\right)}{\sinh\mu_3} + \frac{\left(f_{o(p)}(1)e^{-1/2(1-\eta)}\ \sinh\mu_3\eta\right)}{\sinh\mu_3}$$
$$-f_{o(p)}(0)e^{-(\mu_3+\eta/2)} + f_{o(p)}(\eta) \tag{44}$$

and for the downstream region

$$\Theta_1(\eta)=\frac{\gamma_1\Theta_w e^{\frac{1}{2}(\alpha x-\eta)}\sinh\mu_1\eta}{\sinh(\mu_1\alpha x)}-\frac{\Theta_{1(p)}(\alpha x)e^{-\frac{1}{2}(\alpha x-\eta)}\sinh\mu_1\eta}{\sinh(\mu_1\alpha x)}$$

$$+\frac{\Theta_{1(p)}(0)e^{-(\mu\alpha x+\eta/2)}\sinh\mu_1\eta}{\sinh(\mu_1\alpha x)}-\Theta_{1(p)}(0)e^{-(\alpha x-(\mu_1+1/2)\eta\ )}+\Theta_{1(p)}(\eta) \qquad (45)$$

$$\Phi_1(\eta)=\frac{\gamma_2\Phi_w e^{\frac{1}{2}(\alpha x-\eta)}\sinh\mu_2\eta}{\sinh(\mu_2\alpha x)}+\frac{\Phi_{1(p)}(\alpha x)e^{-\frac{1}{2}(\alpha x-\eta)}\sinh\mu_2\eta}{\sinh(\mu_2\alpha x)}$$

$$+\frac{\Phi_{1(p)}(0)e^{-(\mu\alpha x+\eta/2)}\sinh\mu_2\eta}{\sinh(\mu_2\alpha x)}-\Phi_{1(p)}(0)e^{-(\alpha x-(\mu_2+1/2)\eta\ )}+\Phi_{1(p)}(\eta) \qquad (46)$$

$$f_1(\eta)=\frac{f_{1(p)}(0)e^{-(\mu_3\alpha x+\eta/2)}\sinh\mu_3\eta}{\sinh\mu_3\alpha x}+\frac{f_{1(p)}(\alpha x)e^{1/2(\alpha x-\eta)}\sinh\mu_3\eta}{\sinh(\mu_3\alpha x)}$$

$$-f_{1(p)}(0)e^{(\alpha x-(\mu_{3+1/2})\eta)}+f_{1(p)}(\eta) \qquad (47)$$

3 RESULTS

Using the following realistic and constant values of $\gamma_1 = 0.6$, $\gamma_2 = 0.6$, $\Phi_w = 2.0$, $\Theta_w = 2.0$, $Pe_h = 0.07$, $Pe_m = 0.07$, Re= 400, Gr = 0.1, Gc = 0.1, $\delta_1^2 = 0.2$, $N^2 = 0.2$, $\chi^2 = 0.2$ and varied values of α, Re and M^2, we have the follow results:

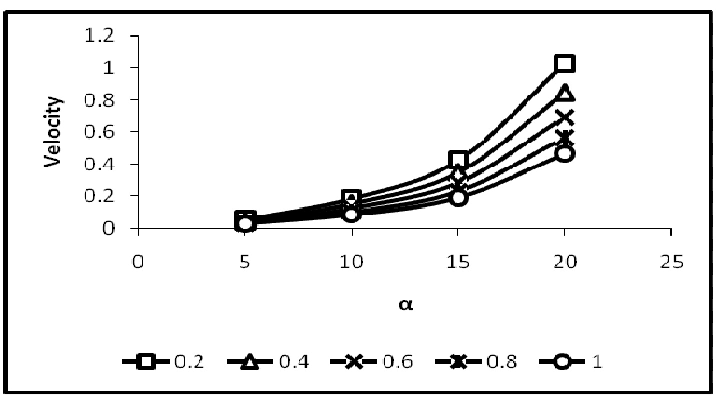

Fig .2 Velocity profiles for various bifurcation angles (α) in the downstream region

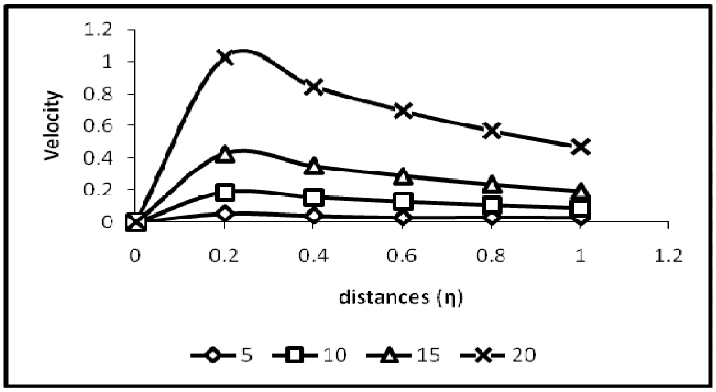

Fig. 3 Velocity -bifurcation angle (α) profiles at various distances (η) in the downstream region.

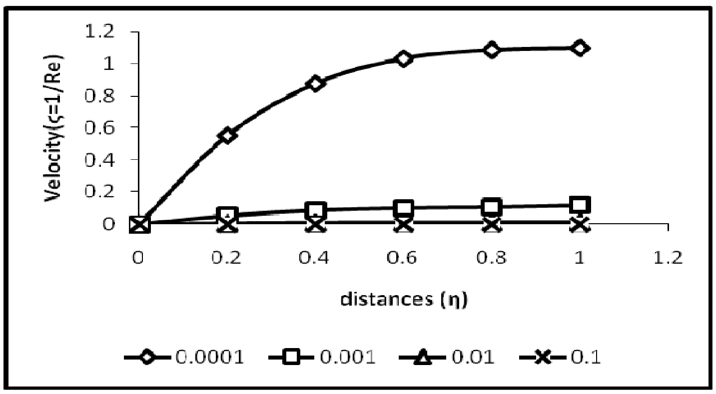

Fig 4 Velocity-Reynolds number (Re) profiles at various distances (η) in the downstream region.

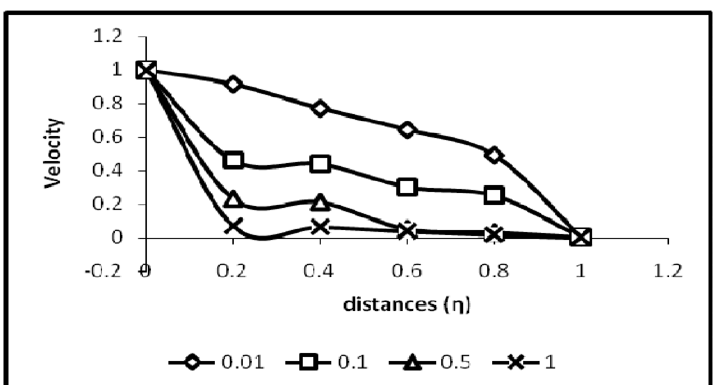

Fig 5 Velocity-magnetic field parameter (M^2) profiles at various distances (η) in the upstream region

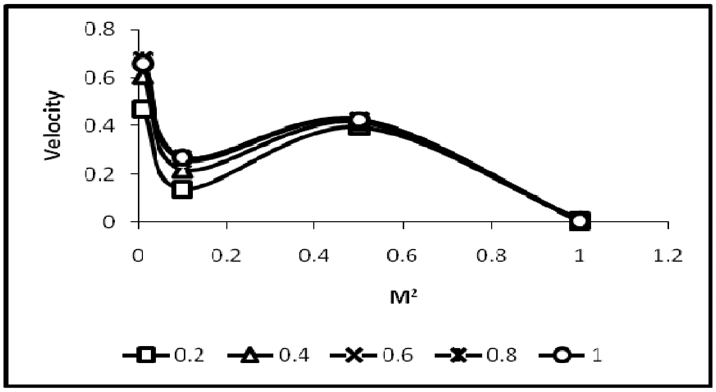

Fig 6 Velocity profiles for various magnetic field parameter (M^2) in the downstream region

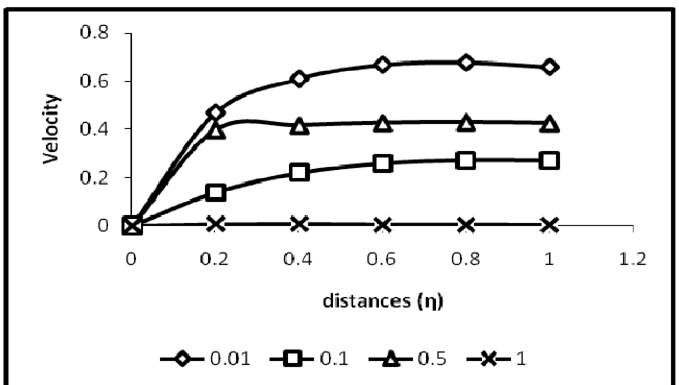

Fig 7 Velocity-magnetic field parameter (M^2) profiles at various distances (η) in the downstream region

4 DISCUSSION

The purpose of this present paper is to investigate the effects of bifurcation angle and magnetic field on the flow. To this end, Fig.2 – Fig.7 illustrate the effects of bifurcation angle, Reynolds number and magnetic field on the transport of water in a stream. The results obtained, show that, for varied values of α, Re and M^2 the transport velocity increases as α and Re increase (Fig.2, Fig.3 and Fig.4) but decreases in the upstream region as M^2 increases (Fig.5). Furthermore so, the velocity oscillates and fluctuates in the downstream region as M^2 increases (Fig. 6 and Fig.7).

An increase in the angle of bifurcation narrows the width of the stream, which in turn increases the inlet pressure in the downstream region with consequent increase in the velocity flow structure as seen in Fig.2 and Fig.3. This agrees with [8], [9], [10], [11], [12], [13], [14].

More so, the flow in the upstream region is laminar and Poiseuille; therefore, its Re is moderate. But, almost at the point of bifurcation or the entry point of the downstream region, the flow exhibits some oscillatory behaviour in the upstream due to a change in geometrical configuration. At this point, the inertial force rises, leading to a drastic increase in the Re, indicating a sort of turbulent flow. This accounts for what is seen in Fig.4. As the Re increases the velocity increases and the water rushes into the downstream region with a great force. The flow regains its laminar nature some distance away from the entry region.

Similarly, the source rocks in the mountain may be made of metallic oxides and salts which dissolve in the water to make it alkaline or saline. Then, the water becomes electrolytic, and therefore, exists as charges. The action of the earth magnetic field on the charges produces a mechanical force, the Lorentz force, which gives the flow new orientations. In particular, the Lorentz force has a freezing impact on the velocity flow structure, thus accounting for what is seen in Fig.5.

Also, the oscillatory and fluctuating motion, manifested in the form of back- and-forth movement of the water, as seen in Figure 6 and Figure 7, possibly, in addition, may be due to the internal waves developed in the water in the flow process, or may be caused by the interaction between the pressure forces and the gravity forces.

The increase and decrease in velocity, coupled with the oscillatory motion in the downstream have tremendous implications. The drastic increase in velocity at the inlet of the downstream channel leads to lateral washing away of the embankment, and makes for navigation risky; the increase in the velocity enhances the transfer of sediments towards the standing water body ahead of it. On the other hand, the decrease in velocity gives room for early deposition of sediments on its bed, and this tends to shallow-up the stream earlier; the oscillatory motion of the fluid at the early stage leads to loss of energy for the flow, and also makes navigation risky.

5 CONCLUSION

The analyses of the flow model show that the velocity increases with bifurcation angle and Reynolds number, while magnetic field freezes the motion in the upstream region, and makes it oscillatory in the downstream region. The increase in the velocity enhances the transport of its bed loads farther towards the mouth of the standing water body and saves it from early deposition and shallow-up. The effects of bifurcation angle and Reynolds number tends to cushion the adverse effects of magnetic field on the flow.

REFERENCES

[1] Makaske Bart. Anastomosing rivers: a review of their classification, origin and sedimentary products. Earth Science Review, 2001; 53:149 – 196

[2] Gary Nichols. Sedimentology and Stratigraphy, 2nd Edition, Wiley-Blackwell Publishers, USA; 2009.

[3] Hoey T. Temporal variations in bed load transport rate and sediment storage in gravel -bed rivers, Prog. Physical Geography. 1992; 16(3): 319 – 338.

[4] Singh VP. Hydrologic systems: volume 1, Rainfall - run-off modeling, Prentice House, Englewood Cliffs, New Jessey; 1988

[5] Singh VP. Kinematic wave modeling in water resources, surface water hydrology, John Wiley and Sons, New York; 1996

[6] Marusic Galino. A study on the mathematical modeling of water quality in river-type aquatic system, WSEAS Transactions on Fluid Mechanics. 2013; 80 – 89.

[7] Tung T vu, Phuoc KT Nguyem, Lioyd HC Chua, Adrian WK Law. Two-dimensional hydrodynamical modeling of flood inundation for a part of the River Mekong with TELEMAC-2D. British J Environment and climatic change. 2015; 5(2): 162-175.

[8] Smith FT. Steady flow through a branching tube, Process Soc. London. 1977; A355:167-187.

[9] Sobey J, Philip Drazin G. Bifurcating two- dimensional flow, J Fluid Mechanics. 1986; 171: 263 -287.

[10] Smith FT, Jones MA. One-to-few and one-to-many branching tube flow, Journal of Fluid Mechanics. 2000; 423: 1–32.

[11] Smith FT, Jones MA. Modeling of multi–branching tube flows: Large flow rates and dual solutions. IMA J Mathematical Medical Biology. 2003; 20: 183–204.

[12] Smith FT, Ovenden NC, Frank P, Doorly DJ. What happens to pressure when a fluid enters a side branch. J Fluid Mechanics. 2003; 479: 231–258.

[13] Pittaluga MB, Repetto R, Tubino M. Channel bifurcation in braided rivers: equilibrium configuration and stability. Water Resources Research. 2003; 39(3): 1046 – 57.

[14] Tadjfar M, Smith FT. Direct simulation and modeling of a 3- dimensional bifurcating tube flow. J Fluid Mechanics. 2004; 519: 1- 32.

[15] Bestman AR. Global models for the biomechanics of green plants, Part 1, International J Energy Research. 1991; 16: 677– 84.

APPENDICES

$$f_{o(p)}(\eta)=-\left(\frac{n_3}{n_3\left(n_3^2-n_2n_3\right)}-\frac{1}{\left(n_3^2-n_2n_3\right)}\right)\left(\frac{GrAe^{\lambda_1\eta}}{\lambda_1}+\frac{GrBe^{\lambda_2\eta}}{\lambda_2}+\frac{GrCe^{m_1\eta}}{m_1}+\frac{GrDe^{m_2\eta}}{m_2}\right)$$

$$+\frac{n_3}{n_3\left(n_3^2-n_2n_3\right)}\left(\frac{GrAe^{\lambda_1\eta}}{(\lambda_1-n_2)}+\frac{GrBe^{\lambda_2\eta}}{(\lambda_2-n_2)}+\frac{GrCe^{m_1\eta}}{(m_1-n_2)}+\frac{GrDe^{m_2\eta}}{(m_2-n_2)}\right)$$

$$-\frac{1}{n_3\left(n_3^2-n_2n_3\right)}\left(\frac{GrAe^{\lambda_1\eta}}{(\lambda_1-n_3)}+\frac{GrBe^{\lambda_2\eta}}{(\lambda_2-n_3)}+\frac{GrCe^{m_1\eta}}{(m_1-n_3)}+\frac{GrDe^{m_2\eta}}{(m_2-n_3)}\right)$$

$$\lambda_1=-\frac{1}{2}+\frac{\sqrt{1-4N^2}}{2},\ \lambda_2=-\frac{1}{2}-\frac{\sqrt{1-4N^2}}{2}$$

$$\lambda_1=-\frac{1}{2}+\mu_1,\lambda_2=-\frac{1}{2}-\mu_1,\mu_1=\frac{\sqrt{1-4N^2}}{2}$$

$$m_1=-\frac{1}{2}+\mu_2,m_2=-\frac{1}{2}-\mu_2,\mu_2=\frac{\sqrt{1-4\delta_1^2}}{2}$$

$$n_2=-\frac{1}{2}+\mu_3,n_3=-\frac{1}{2}-\mu_3,\mu_3=\frac{\sqrt{1-4M^2}}{2}$$

$$A=\frac{\Theta_w e^{1/2}-e^{\mu_1}}{\sinh\mu_1},B=\frac{e^{\mu_1}-\Theta_w e^{1/2}}{\sinh\ \mu_1},\ C=\frac{\Phi_w e^{1/2}-e^{\mu_2}}{\sinh\mu_2},D=\frac{e^{\mu_2}-\Phi_w e^{1/2}}{\sinh\mu_2}$$

$$\Theta_{1(p)}(\eta)=\frac{\Pr}{(\lambda_2-\lambda_1)}\Big[\ \lambda_1FAe^{(\lambda_1+n_2)\eta}+\lambda_1GAe^{(\lambda_1+n_3)\eta}$$

$$-\left(\frac{n_3}{n_2\left(n_3^2-n_2n_3\right)}-\frac{1}{\left(n_3^2-n_2n_3\right)}\right)\left(GrA^2e^{2\lambda_1\eta}+\frac{\lambda_1GrABe^{(\lambda_1+\lambda_2)\eta}}{\lambda_2}+\frac{\lambda_1GcACe^{(\lambda_1+m_1)\eta}}{m_1}+\frac{\lambda_1GcADe^{(\lambda_1+m_2)\eta}}{m_2}\right)$$

$$+\frac{n_3}{n_2\left(n_3^2-n_2n_3\right)}\left(\frac{\lambda_1GrA^2e^{2\lambda_1\eta}}{(\lambda_1-n_2)}+\frac{\lambda_1GrABe^{(\lambda_1+\lambda_2)\eta}}{(\lambda_2-n_2)}+\frac{\lambda_1GcACe^{(\lambda_1+m_1)\eta}}{(m_1-n_2)}+\frac{\lambda_1GcADe^{(\lambda_1+m_2)\eta}}{(m_2-n_2)}\right)$$

$$-\frac{1}{\left(n_3^2-n_2n_3\right)}\left(\frac{\lambda_1GrA^2e^{2\lambda_1\eta}}{(\lambda_1-n_3)}+\frac{\lambda_1GrABe^{(\lambda_1+\lambda_2)\eta}}{(\lambda_2-n_3)}+\frac{\lambda_1GcACe^{(\lambda_1+m_1)\eta}}{(m_1-n_3)}+\frac{\lambda_1GcADe^{(\lambda_1+m_2)\eta}}{(m_2-n_3)}\right)\ \Big]+\ldots$$

$$\Phi_{1(p)}(\eta)=\frac{Sc}{(m_2-m_1)}\Big[\ m_1FCe^{(m_1+n_2)\eta}+m_1GCe^{(m_1+n_3)\eta}$$

$$-\left(\frac{n_3}{n_2\left(n_3^2-n_2n_3\right)}-\frac{1}{\left(n_3^2-n_2n_3\right)}\right)\left(\begin{array}{l}\dfrac{m_1GrACe^{(\lambda_1+m_1)\eta}}{\lambda_1}+\dfrac{m_1GrBCe^{(\lambda_2+m_1)\eta}}{\lambda_2}+GcC^2e^{2m_1\eta}\\+\dfrac{m_1GcCDe^{(m_1+m_2)\eta}}{m_2}\end{array}\right)$$

$$+\frac{n_3}{n_2\left(n_3^2-n_2n_3\right)}\left(\frac{m_1GrACe^{(\lambda_1+m_1)\eta}}{(\lambda_1-n_2)}+\frac{m_1GrBCe^{(\lambda_2+m_1)\eta}}{(\lambda_2-n_2)}+\frac{m_1GcC^2e^{2m_1\eta}}{(m_1-n_2)}+\frac{m_1GcCDe^{(m_1+m_2)\eta}}{(m_2-n_2)}\right)$$

$$-\frac{1}{\left(n_3^2-n_2n_3\right)}\left(\frac{m_1GrACe^{(\lambda_1+m_1)\eta}}{(\lambda_1-n_3)}+\frac{m_1GrBCe^{(\lambda_2+m_1)\eta}}{(\lambda_2-n_3)}+\frac{m_1GcC^2e^{2m_1\eta}}{(m_1-n_3)}+\frac{m_1GcCDe^{(m_1+m_2)\eta}}{(m_2-n_3)}\right)\Big]+\ldots$$

$$-Gr\ \left\{\frac{J_1e^{n_1\eta}}{n_2}+\frac{J_2e^{n_2\eta}}{n_2}\right.+\frac{\Pr}{(\lambda_2-\lambda_1)}\Big[\frac{\lambda_1FAe^{(\lambda_1+n_2)\eta}}{(\lambda_1+n_2)}+\frac{\lambda_1GAe^{(\lambda_1+n_3)\eta}}{(\lambda_1+n_3)}$$

$$-\left(\frac{n_3}{\left(n_3^2-n_2n_3\right)}-\frac{1}{\left(n_3^2-n_2n_3\right)}\right)\left(\frac{GrA^2e^{2\lambda_1\eta}}{2}+\frac{GrBAe^{(\lambda_1+\lambda_2)\eta}}{(\lambda_1+\lambda_2)}+\frac{\lambda_1GcCAe^{(\lambda_1+m_1)\eta}}{(\lambda_1+m_1)m_1}+\frac{\lambda_1GcDAe^{(\lambda_1+m_2)\eta}}{(\lambda_1+m_2)m_2}\right)$$

$$+\frac{n_3}{n_2\left(n_3^2-n_2n_3\right)}\left(\frac{GrA^2e^{2\lambda_1\eta}}{2(\lambda_1-n_2)}+\frac{\lambda_1GrBAe^{(\lambda_1+\lambda_2)\eta}}{(\lambda_2-n_2)(\lambda_1+\lambda_2)}+\frac{\lambda_1GcCAe^{(\lambda_1+m_1)\eta}}{(m_1-n_2)(\lambda_1+m_1)}+\frac{\lambda_1GcDAe^{(\lambda_1+m_2)\eta}}{(m_2-n_2)(\lambda_1+m_2)}\right)$$

$$-\frac{1}{\left(n_3^2-n_2n_3\right)}\left(\frac{GrA^2e^{2\lambda_1\eta}}{2(\lambda_1-n_3)}+\frac{\lambda_1GrBAe^{(\lambda_1+\lambda_2)\eta}}{(\lambda_2-n_3)(\lambda_1+\lambda_2)}+\frac{\lambda_1GcCAe^{(\lambda_1+m_1)\eta}}{(m_1-n_3)(\lambda_1+m_1)}+\frac{\lambda_1GcDAe^{(\lambda_1+m_2)\eta}}{(m_2-n_3)(\lambda_1+m_2)}\right)\Big]+\ldots\}$$

$$f_{1(p)}(\eta)=\left(\frac{n_3}{n_2\left(n_3^2-n_2n_3\right)}-\frac{1}{\left(n_3^2-n_2n_2\right)}\right)\ \Big\{\ \Big[Fe^{n_2\eta}+Ge^{n_3\eta}$$

$$-\left(\frac{n_3}{n_2\left(n_3^2-n_2n_3\right)}-\frac{1}{\left(n_3^2-n_2n_3\right)}\right)\left(\frac{GrAe^{\lambda_1\eta}}{\lambda_1}+\frac{GrBe^{\lambda_2\eta}}{\lambda_2}+\frac{GcCe^{m_1\eta}}{m_1}+\frac{GcDe^{m_2\eta}}{m_2}\right)$$

$$+\frac{n_3}{n_2\left(n_3^2-n_2n_3\right)}\left(\frac{GrAe^{\lambda_1\eta}}{(\lambda_1-n_2)}+\frac{GrBe^{\lambda_2\eta}}{(\lambda_2-n_2)}+\frac{GcCe^{m_1\eta}}{(m_1-n_2)}+\frac{GcDe^{m_2\eta}}{(m_2-n_2)}\right)$$

$$-\frac{1}{\left(n_3^2-n_2n_3\right)}\left(\frac{GrAe^{\lambda_1\eta}}{\left(\lambda_1-n_3\right)}+\frac{GrBe^{\lambda_2\eta}}{\left(\lambda_2-n_3\right)}+\frac{GcCe^{m_1\eta}}{\left(m_1-n_3\right)}+\frac{GcDe^{m_2\eta}}{\left(m_2-n_3\right)}\right)\;]+\ldots$$

$$-\frac{1}{\left(n_3^2-n_2n_3\right)}\left(\frac{GrAe^{\lambda_1\eta}}{\left(\lambda_1-n_3\right)}+\frac{GrBe^{\lambda_2\eta}}{\left(\lambda_2-n_3\right)}+\frac{GcCe^{m_1\eta}}{\left(m_1-n_3\right)}+\frac{GcDe^{m_2\eta}}{\left(m_2-n_3\right)}\right)\;]$$

$$-\left(\frac{n_3}{\left(n_3^2-n_2n_3\right)}-\frac{1}{\left(n_3^2-n_2n_3\right)}\right)\left(\frac{GrA^2e^{2\lambda_1\eta}}{2}+\frac{GrBAe^{(\lambda_1+\lambda_2)\eta}}{\left(\lambda_1+\lambda_2\right)}+\frac{\lambda_1GcCAe^{(\lambda_1+m_1)\eta}}{\left(\lambda_1+m_1\right)m_1}+\frac{\lambda_1GcDAe^{(\lambda_1+m_2)\eta}}{\left(\lambda_1+m_2\right)m_2}\right)$$

$$+\frac{n_3}{n_2\left(n_3^2-n_2n_3\right)}\left(\frac{GrA^2e^{2\lambda_1\eta}}{2\left(\lambda_1-n_2\right)}+\frac{\lambda_1GrBAe^{(\lambda_1+\lambda_2)\eta}}{\left(\lambda_2-n_2\right)\left(\lambda_1+\lambda_2\right)}+\frac{\lambda_1GcCAe^{(\lambda_1+m_1)\eta}}{\left(m_1-n_2\right)\left(\lambda_1+m_1\right)}+\frac{\lambda_1GcDAe^{(\lambda_1+m_2)\eta}}{\left(m_2-n_2\right)\left(\lambda_1+m_2\right)}\right)$$

$$-\frac{1}{\left(n_3^2-n_2n_3\right)}\left(\frac{GrA^2e^{2\lambda_1\eta}}{2\left(\lambda_1-n_3\right)}+\frac{\lambda_1GrBAe^{(\lambda_1+\lambda_2)\eta}}{\left(\lambda_2-n_3\right)\left(\lambda_1+\lambda_2\right)}+\frac{\lambda_1GcCAe^{(\lambda_1+m_1)\eta}}{\left(m_1-n_3\right)\left(\lambda_1+m_1\right)}+\frac{\lambda_1GcDAe^{(\lambda_1+m_2)\eta}}{\left(m_2-n_3\right)\left(\lambda_1+m_2\right)}\right)\;]$$

$$+\ldots\quad -Gc\;\left\{\frac{\mathrm{R}_1e^{m_1\eta}}{m_1}+\frac{\mathrm{R}_2e^{m_2\eta}}{m_2}\quad+\frac{Sc}{\left(m_2-m_1\right)}\left[\frac{m_1FCe^{(m_1+n_2)\eta}}{\left(m_1+n_2\right)}+\frac{m_1GCe^{(m_1+n_3)\eta}}{\left(m_1+n_3\right)}\right.\right.$$

$$\left(\frac{n_3}{n_2\left(n_3^2-n_2n_3\right)}-\frac{1}{\left(n_3^2-n_2n_3\right)}\right)\left(\frac{m_1GrACe^{\left(m_1+\lambda_1\right)\eta}}{\lambda_1\left(m_1+\lambda_1\right)}+\frac{m_1GrBCe^{\left(m_1+\lambda_1\right)\eta}}{\lambda_2\left(m_1+\lambda_1\right)}+\frac{GcC^2e^{2m_1\eta}}{2m_1}+\frac{m_1GcDCe^{\left(m_1+m_2\right)\eta}}{m_2\left(m_1+m_2\right)}\right)$$

$$-\frac{n_3}{n_2\left(n_3^2-n_2n_3\right)}\left(\frac{m_1GrACe^{\left(m_1+\lambda_1\right)\eta}}{\left(\lambda_1-n_2\right)\left(m_1+\lambda_1\right)}+\frac{m_1GrBCe^{\left(m_1+\lambda_2\right)\eta}}{\left(\lambda_2-n_2\right)\left(m_1+\lambda_2\right)}+\frac{GcC^2e^{2m_1\eta}}{\left(m_1-n_2\right)2}+\frac{m_1GcDCe^{\left(m_1+m_2\right)\eta}}{\left(m_2-n_2\right)\left(m_1+m_2\right)}\right)$$

$$-\frac{1}{\left(n_3^2-n_2n_3\right)}\left(\frac{m_1GrACe^{(m_1+\lambda_1)\eta}}{\left(\lambda_1-n_3\right)\left(m_1+\lambda_1\right)}+\frac{m_1GrBCe^{(m_1+\lambda_2)\eta}}{\left(\lambda_2-n_3\right)\left(m_1+\lambda_2\right)}+\frac{GcC^2e^{2m_1\eta}}{\left(m_1-n_3\right)2}+\frac{m_1GcDCe^{(m_1+m_2)\eta}}{\left(m_2-n_3\right)\left(m_1+m_2\right)}\right)\;]+\ldots]\}$$

$$E=0$$

$$F=\frac{\left(\;f_{o(p)}(0)e^{-(\mu_3+1/2)}-f_{o(p)}(1)\right)e^{1/2}}{2\sinh\mu_3},$$

$$G=\frac{-\left(\;f_{o(p)}(0)e^{-(\mu_3+1/2)}-f_{o(p)}(1)\right)e^{1/2}}{2\sinh\mu_3}-f_{o(p)}(0)$$

$$J_1 = \frac{e^{\alpha x/2}\left(\gamma_1\Theta_w - \Theta_{1(p)}\left(\alpha x\right) + \Theta_{1(p)}\left(0\right)e^{-(\mu_1+1/2)\alpha x}\right)}{2\sinh(\mu_1 \alpha x)},$$

$$J_2 = \frac{-e^{\alpha x/2}\left(\gamma_1\Theta_w - \Theta_{1(p)}\left(\alpha x\right) + \Theta_{1(p)}\left(0\right)e^{-(\mu_1+1/2)\alpha x}\right)}{2\sinh(\mu_1 \alpha x)} - \Theta_{1(p)}\left(0\right)$$

$$R_1 = \frac{e^{\alpha x/2}\left(\gamma_2\Phi_w - \Phi_{1(p)}\left(\alpha x\right) + \Phi_{1(p)}\left(0\right)e^{-(\mu_2+1/2)\alpha x}\right)}{2\sinh(\mu_2 \alpha x)},$$

$$R_2 = \frac{-e^{\alpha x/2}\left(\gamma_2\Phi_w - \Phi_{1(p)}\left(\alpha x\right) + \Phi_{1(p)}\left(0\right)e^{-(\mu_2+1/2)\alpha x}\right)}{2\sinh(\mu_2 \alpha x)} - \Phi_{1(p)}\left(0\right)$$